In situ seed-growth synthesis of silver nanoplates on glass for the detection of food contaminants by surface enhanced Raman scattering

Talanta 216 (2020) 120936

Contents lists available at ScienceDirect

Talanta

journal homepage: www.elsevier.com/locate/talanta

In situ seed-growth synthesis of silver nanoplates on glass for the detection of food contaminants by surface enhanced Raman scattering

Agnese D'Agostino[a], Andrea Mario Giovannozzi[b,*], Luisa Mandrile[b], Alessio Sacco[b], Andrea Mario Rossi[b], Angelo Taglietti[a,**]

[a] Dipartimento di Chimica, Sezione di Chimica Generale, Università di Pavia, viale Taramelli, 12, 27100, Pavia, Italy
[b] Istituto Nazionale di Ricerca Metrologica (INRiM), Strada delle Cacce 91, 10135, Torino, Italy

ARTICLE INFO

Keywords:
SERS
Silver nanoplates
Seed-growth synthesis
Pesticides
Thiram
PLS

ABSTRACT

Seed-growth synthesis is a common strategy to prepare silver nanoplates, whose peculiar plasmonic features can be exploited for surface enhanced Raman scattering (SERS) applications. Here we describe the fabrication and characterization of SERS chips using a peculiar *in situ* seed growth method, yielding a dense layer of nano-objects directly on a glass slide. In this way, geometric features (i.e. shape and dimensions) of the nano-objects can be tuned by controlling the growth time, obtaining a high concentration of hot spots on the surface. In particular, the SERS response of four kinds of chips were investigated to define the best SERS configuration in terms of size of the silver nano-objects, excitation wavelength and homogeneity of the SERS response. Silver nano-plates with a seeded growth time of 60 min demonstrated remarkable results both in terms of plasmonic enhancement, with an enhancement factor (EF) of 2×10^5 using a 532 nm laser excitation, and good homogeneity of the SERS response with intra- and inter-maps RSD of 10% and 5%, respectively. In order to demonstrate application of these chips for real sample analysis, an analytical procedure for the detection of a model pesticide, i.e. thiram fungicide, was developed and applied to its detection on green apples peels. SERS measurements on 60 min seeded growth silver nano-plates chip coupled with a multivariate PLS approach demonstrated high accuracy and repeatability for thiram detection in food matrix within the European law limits.

1. Introduction

Surface Enhanced Raman spectroscopy (SERS) has seen an enormous increase of popularity in various application, due to its intriguing feature to signal the presence of chemical species by the vibrational fingerprint together with a huge enhancement of Raman signal. This allowed successful applications ranging from materials science [1], biomedical imaging [2,3] to food safety [4].

In order to prepare optimal SERS substrates as sensing chips for analytical applications, some features must be provided, such as high sensitivity, uniformity of the enhancement factor (EF) on the overall extension of chip surfaces, good mechanical and chemical stability, good reproducibility, low cost and easy synthetic pathway [5,6]. The successes obtained in increasing the values of EFs lead to the exploitation of anisotropic metal nano-objects of various shapes [7,8]. As it was widely demonstrated [8,9], the EF increases intensely when molecules are close to tips and sharp edges of properly shaped NP, due to the "lightning rod effect", or inside the gaps among clusters of metallic nano-objects called "hot spots". In these zones, thank to electromagnetic (EM) field confinement, enhanced signals can raise of a factor up to 10^{12}–10^{13} compared to the intensities which are usually found in classical Raman measures [10,11].

Silver nanoplates have demonstrated to act as very effective starting NP to boost the EF. They indeed have sharp edges and can be easily arranged in bi-dimensional arrays producing a high surface concentration of hot spots. Several studies were reported on the use of silver nanoplates organized on a surface. In some cases, nanoparticles were previously synthesized and then attached to the proper substrate to obtain the sensing chip [12–14]. In other examples, silver nanoplates or other plate-like nanoparticles were grown directly on the desired surface through *in-situ* or seed-mediated methods and applied in SERS detection of different target molecules [15–20]. Anyway, some issues related to the production of reliable SERS chips are still a challenge: for instance, the control of homogeneity and reproducibility of the preparations, the optimization of the conditions needed to obtain a dense coating to ensure a maximization of hot spots [21], the reproducibility

* Corresponding author.
** Corresponding author.
E-mail addresses: a.giovannozzi@inrim.it (A.M. Giovannozzi), angelo.taglietti@unipv.it (A. Taglietti).

https://doi.org/10.1016/j.talanta.2020.120936
Received 23 December 2019; Received in revised form 12 March 2020; Accepted 14 March 2020
Available online 19 March 2020
0039-9140/

of SERS spectra. A successful example comes from Khlebtsov and colleagues, who realized films of gold nanoislands with tuneable morphology grafted on glass or silicon substrates, using a seed-growth method, starting from a layer of small gold nanoparticles: they obtained high EF and reproducibility for a model compound (4-aminothiophenol) and encouraging data on the detection of thiram fungicide in apple peels [22].

In this work, we propose a way to prepare SERS chips based on silver nanoplates, tailored to have a high localized surface plasmon resonance (LSPR) extinction and a dense and homogeneous array hot spots, thus efficient and reproducible SERS responses. Recently, we introduced a seed-growth synthetic method which can be used to prepare silver nano-plates layers directly on the desired surfaces, simply using citrate anions to direct the anisotropic growth [23]. Using this method it is possible to tune the geometric features (i.e. shape and dimensions) of the nano-objects controlling the growth time: within this approach the scope of this work is to find the optimal conditions to give high SERS effects on a model compound (7-mercapto-4-methylcoumarin, MMC) which has been found to be a good Raman reporter [24,25] and then move to the detection of the fungicide thiram in a real sample matrix, i.e. pome fruits, after extraction from the surface of the fruit.

2. Materials and methods

2.1. Chemicals

Silver nitrate (> 99.8%), sodium borohydride (> 99.0%), sodium citrate (> 99.0%), ascorbic acid (≥99%), 7-mercapto-4-methylcoumarin (> 97%) were purchased from Sigma Aldrich. Trimethoxysilylpropyl(polyethylenimine) (50% in isopropanol) was purchased from Gelest Inc. Tetramethylthiuram disulfide, (97%) was purchased from Alfa Aesar. Ethanol (≥99%, spectroscopic grade) was purchased from Carlo Erba. Reagents and solvents were used as received.

Microscopy cover glass slides 21 × 26 mm have been obtained from DEL Chimica. Water was deionized and double distilled (ddH2O). Glassware was cleaned with aqua regia carefully, and after this was washed three times with ddH2O water for 3 min under sonication, before use.

2.2. Preparation of SERS chips

We prepared the chips following a previously reported method [23]. Full details of sample preparation are reported in ESI. Briefly, pretreated glass slides were dipped in a 4% (v/v) solution of PEI-silane in ethanol at room temperature for 6 min. Eight samples were prepared in the same time using a hellendhal jar.

Small spherical silver nanoparticles to be used as seeds were synthesized following a reported procedure [23]. Glasses functionalized with PEI were soaked in the suspension of silver nanoparticles (the so called “seeds”) at room temperature for a period of 15 min.

The growth of nanoplates on glass samples was obtained by dipping the glass samples functionalized with the seeds in the proper amount of growth solution, i.e. 30 ml of sodium citrate 0.0085 M, 18 ml of $AgNO_3$ 0.0005 M and 0.450 ml of ascorbic acid 0.01 M.

2.3. UV–vis spectroscopy

UV–Vis spectra of prepared slides at normal incidence were registered in air in the range 350–1100 nm with a spectrophotometer (model: Varian Cary 50 UV/Vis). A dedicated holder, enabling measurement on the same zone of the glass slide samples in every experimental stage, was used.

2.4. Scanning electron microscopy (SEM)

SEM images were obtained using a Tescan Mira XMU variable pressure Field Emission Scanning Electron Microscope – FEG SEM (Tescan USA Inc., USA), located at the Arvedi Laboratory, CISRiC, Pavia. Slides were made electrically conductive by coating them with a thin layer of Pt/Pd (5 nm) while in vacuum. Images were registered with the Backscattered electrons mode (BSE) set at 30 kV and using InBeam secondary electron detector to gain higher spatial resolution.

2.5. Preparation of samples for SERS efficiency and substrate homogeneity test

7-mercapto-4-methylcoumarin (MMC) stock standard solution at 1×10^{-3} M was prepared by diluting 0.192 g of MMC in 1 l of ethanol. MMC standard solutions (1×10^{-6} M, 1×10^{-7} M, 1×10^{-8} M and 1×10^{-9} M) were prepared by subsequent dilutions in ethanol from the stock. SERS efficiency and substrate homogeneity tests were performed by immersing the chips in the standards solution for 1 h, rinsed copiously with ethanol to remove any excess from the surface and then dried with nitrogen before SERS measurements. Pure ethanol was used as blank.

2.6. Preparation of calibration standards

Thiram stock at 1000 mg l^{-1} was prepared in ethanol and subsequently diluted to 100 mg l^{-1}, 10 mg l^{-1}, 1 mg l^{-1}, 0.1 mg l^{-1} and 0.01 mg l^{-1} to set up the analytical procedure.

Thiram standards in fruit matrix were made for Raman spectrometer calibration, as explained in paragraph 2.8. Consecutive dilutions were prepared from 100 mg l^{-1} to obtain the following concentrations in matrix: 7.5 mg l^{-1}, 5.0 mg l^{-1}, 2.5 mg l^{-1}, 1.0 mg l^{-1} and 0 mg l^{-1}.

2.7. Detection of thiram on apples

Pome fruits (green apples) were bought from a local supermarket. Surface of the fruit was thoroughly cleaned with water and sodium bicarbonate, then spiked with thiram to obtain a contaminated surface. Thiram-free apples were processed as the same as spiked apples and used as blanks. Thiram was recovered from the fruit's peel by washing it off from the contaminated surface with a known amount of ethanol. The chips were then immersed in the resulting solution for 1 h, rinsed copiously with ethanol, dried with nitrogen and analyzed by Raman mapping. The amount of thiram on apples was calculated by SERS following to the analytical procedure reported in 2.9.

2.8. Raman measurements

SERS measurements were carried out using a Thermo Scientific™ DXR™ xi Raman Imaging confocal microscope system equipped with different excitation laser sources at 532 nm, 633 nm and 780 nm, gratings with a resolution at 5 cm^{-1} in the spectral range 50 cm^{-1} to 3500 cm^{-1}, a 10× microscope objective, a 50 μm pinhole aperture and an automatic motorized stage.

In the SERS efficiency and substrate homogeneity tests, four maps with a dimension of 500 μm × 500 μm each (25 μm step size) were collected on randomly different locations of the SERS chip. Each spectrum of the map was registered with a laser power of 4 mW using an integration time of 0.01 s (100 Hz) with 20 scans in total.

In the SERS detection of thiram, a single map with a dimension of 50 μm × 50 μm was registered on a random location of the SERS chip, using a laser source at 532 nm. Each spectrum of the map was registered with a laser power of 1 mW using an integration time of 1 Hz with 20 scans in total.

2D-Raman maps were processed with Matlab® for map unfolding and statistical analysis.

2.9. Calibration and validation of the method

Five thiram concentrations in negative matrix pool were used as calibration standards (training set): 0 mg kg^{-1}, 1 mg kg^{-1}, 2.5 mg kg^{-1}, 5 mg kg^{-1}, 7.5 mg kg^{-1}. SERS chips were incubated with these standards and analyzed as described in 2.8. A linear regression was calculated as described in details in ESI. Furthermore, multivariate calibration was performed using Partial Least Square method (Wold H, 2006) using the PLS Toolbox for Matlab® by Eigenvector [26]. Spectral frequencies ranging from 400 cm^{-1} to 1100 cm^{-1} and 2700 cm^{-1} to 3100 cm^{-1} were considered to include the specific peaks of the analyte, neglecting interfering bands. SERS spectra were mean centered before PLS regression. The first model optimization process was performed using a custom cross validation test using the "leave-one concentration-out" strategy. The optimal number of PLS Latent Variables (LVs) was set to 4 on the basis of the cumulative explained variance (CEV = 95.8%). The method was validated, by quantifying a new independent sample, at known concentration of 5 mg kg^{-1}. The root mean square error in prediction RMSEP was used for method precision, while the mean predicted value for method accuracy.

3. Results and discussion

3.1. SERS chips preparation

As we reported earlier [23], the seed growth method here employed can easily yield a homogeneous coating of glass samples with silver nanoplates (AgNPs). An illustrative scheme of the growth mechanism of the AgNPs on glass is shown in Scheme 1.

Small silver nanospheres with diameters close to 7 nm can be obtained by a classical reduction method using sodiumborhydride, and then easily grafted on the PEI functionalized glass slides due to the negative value of the z-potential of seeds (about −25 mV), at the pH of the colloidal suspension (close to value of 6). At this pH, the amino groups of PEI are almost completely protonated, so interaction with the negatively charged seeds is expected. At this point, growth of grafted seeds can be easily obtained placing the samples in a growth chamber filled with a solution of $AgNO_3$, ascorbic acid as mild reductant and citrate as templating (or shape-directing) agent. It is well known that citrate preferentially binds to 111 facets of Ag(0) crystals during their growth, slowing down the vertical expansion due to the reduction of silver ions on Ag(0) crystal surfaces by ascorbic acid, this resulting in the anisotropic growth and production of flat silver nanoplates. We demonstrated that it is possible to obtain increasing anisotropic growth on glass surface just increasing immersion time of grafted seeds in presence of high citrate concentration: control of immersion times allows the tuning of the size and consequently the LSPR features of plasmonic objects on glass samples. These flat nano-objects show an in-plane dipole plasmon resonance band with a shape and a position which usually falls in the NIR region, and which can be tuned at a desired value just by regulating the aspect ratio of the objects. This allows to follow easily the extent of the growth of objects on slides by simply measuring the LSPR spectra after different immersion times [23]. Four growing times at 15 min, 30 min, 60 min and 120 min were investigated.

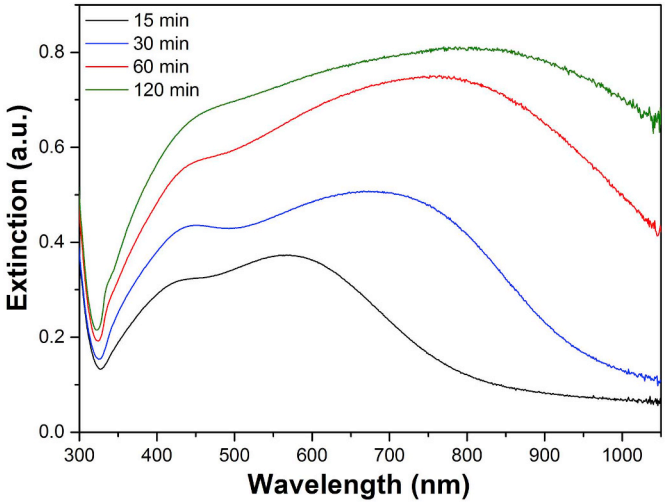

Fig. 1. LSPR spectra registered on glass slides obtained after dipping in growth solution for increasing amounts of time: 15 min (black line), 30 min (blue line), 60 min (red line) and 120 min (green line). (For interpretation of the references to colour in this figure legend, the reader is referred to the Web version of this article.)

Fig. 1 reports the UV-Vis-NIR spectra showing how the progressive red shift of the maximum of the LSPR spectra accounts for the increase of anisotropy and enlargement of plates edges.

SEM images taken on the same substrates and reported in Fig. 2 confirmed a dense and uniform layer of firmly grafted nano-objects, with dimensions and anisotropy increasing with growth time, indicating them as very good candidates for exploitation for SERS purposes.

Short immersion times show the presence of small grafted objects, having spheroidal shapes with 10–20 nm of diameter (15 min, Fig. 2a) and larger discoidal shapes with a size of 20–30 nm (30 min, Fig. 2b). Dimensions and anisotropy clearly increase with growing time, and triangular and truncated triangular plates appear with more evidence for longer immersion times, as a result of the templating action of citrate ions. For 60 min immersion times (Fig. 2c and e) longitudinal dimensions of plates range between 20 and 80 nm, with a thickness close to 15 nm. In case of the longer immersion time (120 min, Fig. 2d) longitudinal dimensions between 40 and 120 nm are reached, with objects still having a thickness not exceeding the value of 20 nm. Due to the random orientation and tilt of nanoplates towards the glass surface,

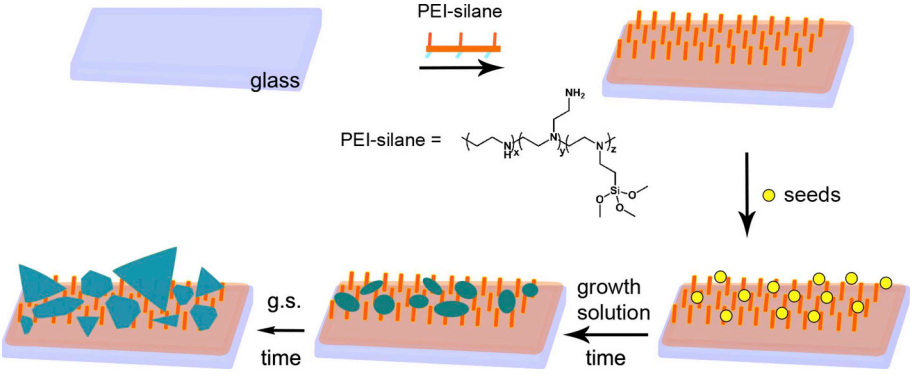

Scheme 1. A schematic representation of the time-dependant seed mediated growth of Ag nanoplates on PEI functionalized glass substrates.

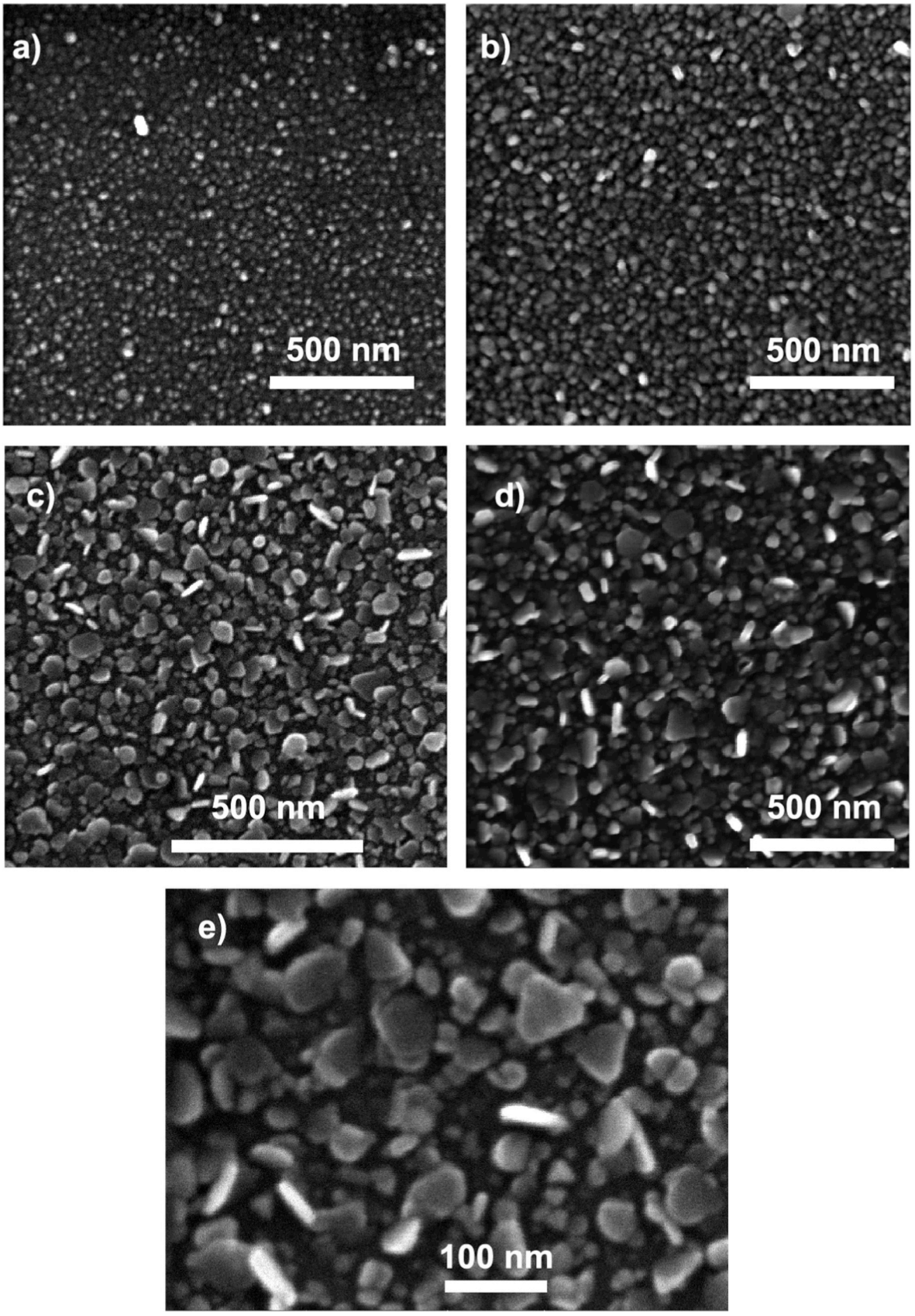

Fig. 2. SEM images of glass obtained after dipping in growth solution for increasing amounts of time: (a) 15 min, (b) 30 min, (c) 60 min, (d) 120 min, (e) 60 min, detail at higher magnification.

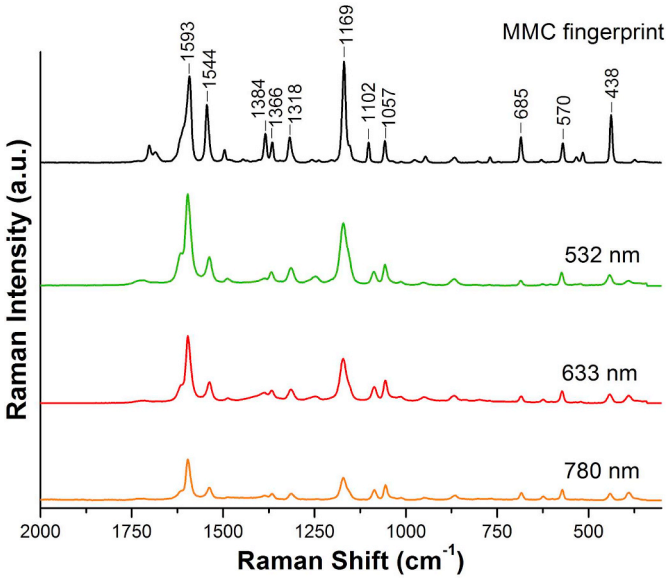

Fig. 3. Conventional Raman spectrum (black line) of MMC in solid state. The average SERS spectra of MMC acquired on the 60 min sample using different laser lines at 532 nm, 633 nm and 780 nm are shown.

and to their crowded arrangement, it was impossible to perform a detailed and more systematic investigation of shapes and dimensions. Nevertheless, the SEM images account for a very homogeneous coating of glass slides with objects having an extremely high degree of polydispersion, and a clear increase of size and anisotropy with the growth time, and this is consistent with the very broad LSPR spectra shifting towards the NIR range observed as growth time increases.

3.2. SERS characterization of the substrates

In order to investigate the SERS response of the four kind of AgNPs SERS chips growth at different time, both in terms of signal enhancement and homogeneity of the response, we decided to use the 7-mercapto-4-methylcoumarin (MMC) as probe molecule. MMC forms a self-assembled-monolayer on the surface of the metallic chips due to the strong covalent bond between the sulphur atom and silver on the substrate, and it provides a well recognizable SERS spectral fingerprint. Conventional Raman spectrum of MMC is shown in Fig. 3, where the main Raman bands are due to the -C-O- stretching mode at 1169 cm^{-1}, to the conjugated –C=C- stretching mode at 1593 cm^{-1}, and to the -C-C- stretching and in-plane deformation of -C-$H_{(ring)}$ at 1543 cm^{-1} [27]. A detailed peak assignment of the MMC is listed in Table S1 in ESI. AgNPs chips were incubated with the MMC and micro-Raman mapping was performed using different laser lines. This study was conducted to evaluate the influence of the LSPRs on the SERS performance and to define the best SERS configuration in terms of size of silver nano-objects, excitation wavelength and homogeneity of the SERS response.

SERS spectra of MMC collected on the 60 min sample using different laser lines are reported in Fig. 3, as an example of the enhancement effect obtained. The obtained spectra show typical MMC features, which are consistent with its traditional Raman spectrum.

As Fig. S1 shows, the enhancement given by different substrates using different laser lines was compared by monitoring the MMC peak at 1593 cm^{-1} over the time of the seed-mediated growth.

In case of the excitation wavelength at 532 nm, the intensity smoothly increases over the growth time reaching the highest value at 120 min. In case of the excitation wavelength at 633 nm and 780 nm, instead, the intensity reaches its maximum after 30 min and 60 min, respectively, and then progressively falls at higher times of growth. SERS performance of these substrates seem to be largely dependent on the LSPR of the silver nano-objects at a given excitation wavelength. When the 633 nm and 780 nm laser lines are used in excitation, the Raman signals were greatly enhanced at 30 min and 60 min, respectively, which corresponds to the close matching of the excitation wavelength to the peak position of LSPR bands (in-plane dipole resonance mode). As soon as we move away from this position by enlarging the size of the nanoplates, the Raman signal start to decrease, probably due to the less effective coupling between the LSPR maximum and the excitation wavelength. Interestingly, a different behavior was registered with the 532 nm excitation, where a continuous slight increase of the Raman signal after 30 min, 60 min and 120 min of the seed-mediated growth was observed. Since the LSPR bands become constantly broader as the size of the plates increases, it is difficult to define which modes are responsible for the continuous increase of the SERS signal, when the 532 nm excitation is used. Other studies on silver nanocubes already suggested the LSPR broadening as the reason for less enhancement variety when the size of the nanocubes increases [28]. The LSPR broadening gives a contribution to the SERS enhancement, probably because the LSPR profile extend to the position of excitation wavelength even though the peak wavelength of LSPR is far away from it [29].

Comparing the SERS performance of the chips using different excitation wavelengths, the 532 nm provided the highest enhancement and it was chosen for further analytical exploitation of these chips. Even if the signal amplification does not change dramatically over the growth time of the plates, the homogeneity of the SERS response seems to provide different results. In order to investigate the homogeneity of differently grown plates, four maps of 0.5 mm^2 were collected for each sample (Figs. S2a–d). In particular, the inter-map homogeneity was evaluated as it represents the variability from map to map within the same substrate [27]. 60 min sample demonstrated the highest homogeneity (1% RSD) of SERS response over wide area. Another important information was also to evaluate the minimum area which provides sufficient repeatability by calculating the RSDs over progressively increasing areas from 1 × 1 μm^2 to 500 × 500 μm^2 (Figs. S3a–g). For every 2D-Raman map, four different regions of the chip were characterized and the results are listed in Table 1.

Increasing the scanned area, the value of the intra-map RSD grew up from 6.8% to 12.3%. RSD values of 20% are usually associated to good homogeneity for SERS substrates [29,30], so the present results indicate high homogeneity of the SERS response of these chips. The inter-maps RSD stays around 10% for quite small areas, while it is lower than 5% for wider areas (from 50 × 50 μm^2 to 500 × 500 μm^2). Our results of about 10% and 5% for the intra-map and inter-maps RSD over 50 × 50 μm^2, respectively, revealed a good homogeneity of the SERS substrate with a remarkable repeatability. These homogeneity and repeatability conditions are suitable for the setup of an accurate analytical procedure.

As the 60 min sample was defined as the best compromise in terms

Table 1
Analysis of SERS substrate homogeneity.

Scanned area (μm^2)	Number of spectra	[a]Intra-map RSD (%)	[a]Inter-maps RSD (%)
1 × 1	1	n/a	11.3
25 × 25	4	6.8	9.2
50 × 50	9	10.8	4.3
125 × 125	36	12.1	3.2
250 × 250	121	12.5	1.6
375 × 375	256	12.4	1.1
500 × 500	441	12.3	0.9

[a] The intra-map RSD is the RSD calculated upon all the spectra composing one Raman map, the reported values are the mean of 4 determinations. The inter-maps RSD is the RSD calculated upon the four intensity averages for each map.

of SERS enhancement and homogeneity of the Raman signal throughout the substrate, we also investigated its sensitivity to diluted concentrations of MMC from 1×10^{-6} M to 1×10^{-9} M concentrations. As the spectra in Fig. S4 show, the specific vibrational bands of the MMC can be clearly detected down to 1×10^{-8} M. Further dilution to 1×10^{-9} M is close to the limit of detection of the substrate, which also shows overlapping of the MMC signals with the bands of the citrate and ascorbic acid from the background, especially in the spectral region 1600-1300 cm^{-1}. The detection of 10 nM concentration represents a good indication of the high substrate sensitivity. An enhancement factor (EF) of 2×10^5 was calculated for the 60 min sample according to the method proposed in Refs. [31] and reported in ESI. Such EF value might not be considered very high if compared to other values reported in literature for other Ag nano-objects [19,20], where EFs in the order of 10^7 - 10^8 were calculated. In other similar Ag SERS systems [16–18], instead, the EF was not reported, and the detection limit of specific target molecules, such as the 2-naphthalenethiol or PCBs, in the micromolar or nanomolar range was only used to evaluate the efficiency of the substrate. In the last case, our Ag-nanoplates chip also showed comparable sensitivity with these previous reported systems with a detection limit of the MMC in the nanomolar range. Moreover, other data reported on gold nanostructures also demonstrated higher SERS performance in terms of EF [32–34]. These SERS substrates were very efficient and provided a more homogenous control of the growth mechanism of the nano-object in terms of size and shape. However, they often employed surfactant molecules that might reduce the adsorption of target molecules for real world application, such as food contaminants, which was indeed not showed in these studies. In general, taking the EF as main parameter to evaluate the efficiency of a SERS system could be misleading. Indeed, a proper comparison between different SERS system should be performed by using the same EF calculation method, the same SERS probe and, more importantly, it should be supported by an accurate calculation of the number of molecules under the laser spot size or in the hot-spot regions, which is normally based on several assumptions. The method applied in this work and previously developed by our group in Ref. [31] tries to push to a standardization of the EF procedure, taking into account the normal issues in the EF calculation. Nonetheless, finding a fair compromise between EF and substrate uniformity is the key element for the fabrication of an excellent SERS substrate. In this way, the system here presented showed excellent homogeneity and reproducibility of the SERS response, thus supporting for real application in food contaminants detection, as the next section will describe.

3.3. SERS detection of thiram on pome fruits

In order to demonstrate application of these chips for real sample analysis, an analytical procedure for the detection of thiram was developed. Tetramethylthiuram disulfide (thiram) is a non-systemic dithiocarbamate fungicide whose residues mostly remain on the surface of the sprayed crop [35]. Maximum allowed levels of thiram residues on fruits and vegetables are in the range 0.1–5 mg kg^{-1}, as defined by the Reg. (EU) 2016/1. Here we describe the setup of an analytical procedure to detect thiram on pome fruits, whose law limit has been set as 5 mg kg^{-1}.

According to the literature, when thiram molecule interacts with a metal surface such as the Ag nanoplate, it easily forms the resonated radical structure that causes the S–S bond cleavage of thiram [36]. This strong adsorption takes place via the SCS group through a bidentate complex with Ag atoms, as shown in Fig. S5a in the ESI [37,38]. A comparison of pure thiram powder and SERS spectra are shown in Fig. S5b. The Raman and SERS spectra contain different vibrational bands, including the one at 564 cm^{-1} attributed to ν(S–S) or ν(CSS), at 1148 cm^{-1} to ρ(CH_3) or ν(N–CH_3), and at 1386 cm^{-1} and at 1514 cm^{-1} to ρ(CH3) and ν(C═N), respectively. The other characteristic vibrational modes for both Raman and SERS spectra are listed in Table S2.

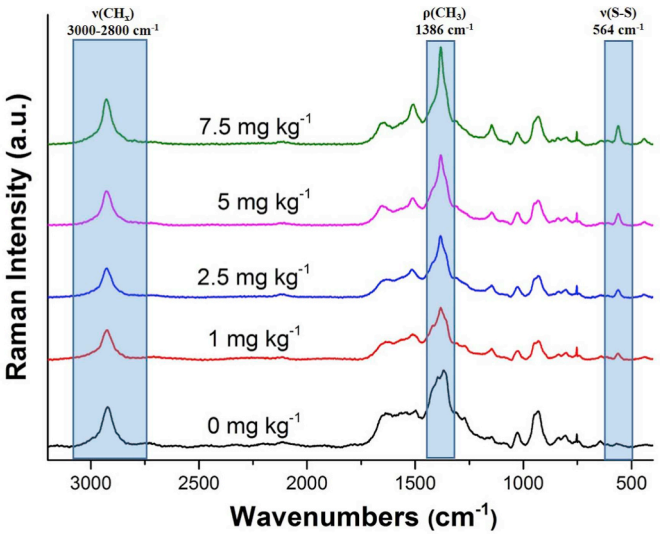

Fig. 4. Average SERS spectra of 60 min silver nanoplates substrates upon incubation with different concentrations of thiram in negative matrix pool, ranging from 0 to 7.5 mg kg^{-1}.

In order to test the sensitivity of the SERS chip, they were incubated for 1 h in thiram solutions ranging from 10 mg l^{-1} to 0.01 mg l^{-1} and then analyzed by Raman mapping. As Fig. S6 shows, the main characteristic bands of thiram at 564 cm^{-1} and 1386 cm^{-1} decrease together with its concentration reaching a detection limit of 0.01 mg kg^{-1}, which is almost one order of magnitude lower than thiram limit residues on fruits and vegetables.

In order to detect and quantify thiram on a real sample, a simple extraction of the pesticide was first performed (paragraph 2.9). An external calibration was carried out to set up the analytical procedure. The average spectrum for each standard was calculated over an area 50×50 μm^2, which is enough to guarantee an intra-map RSD of 5% (Table 1), while reducing the total time of analysis.

As Fig. 4 shows, the specific signals of thiram increase together with the concentration, following a linear trend in the tested range of concentrations. A univariate calibration curve can be built but with limited accuracy (see ESI for details and Fig. S7). A multivariate approach was then used to consider simultaneously the whole information contained in spectral data (Fig. 5). As we previously demonstrated, a multivariate approach provided higher accuracy and method stability than univariate calibration of SERS measurements [39]. A "chemical-shape" is conserved in the loading until LV4 and this was chosen as reasonable model complexity (Fig. S8). A high correlation factor ($R^2_{Cal} = 0.96$) is obtained and maintained during the validation test ($R^2_{CV} = 0.93$). The method provides a RMSECV of 0.7 ppm during the "leave-one concentration-out" validation test using 4 LVs. The external validation test on an independent sample with a real concentration of 5 mg kg^{-1} provided a mean value of 4.5 mg kg^{-1} with a standard deviation of 0.5 mg kg^{-1}. This test allowed to calculate an accuracy of 90.7%. A root mean square error in prediction RMSEP = 0.7 mg kg^{-1} was obtained, which is commonly accepted as an indication of method precision.

In order to test the analytical method for a real application, we used the PLS quantitative method to determine the recovery of thiram from the surface of apples spiked with thiram at 5 mg kg^{-1}. A contamination level of 1.4 ± 0.3 mg kg^{-1} was calculated, averaging 10 measurements. This value demonstrated a recovery of 28%, which means that the extraction procedure only allows to partially recover the contaminant from the apple surface and it will require further

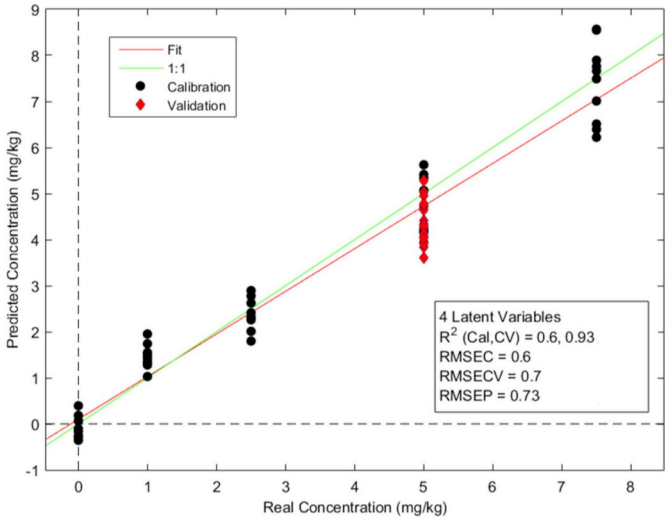

Fig. 5. Measured vs predicted concentration plot for a PLS model of mean centered data, using 5 LVs. Errors and correlation factors are reported in the figure. The red line represents the model trend line to be compared with the optimal 1:1 line in green. (For interpretation of the references to colour in this figure legend, the reader is referred to the Web version of this article.)

improvement. However, this can be considered just a limitation of the preliminary sample processing (i.e. the mild extraction procedure), which does not affect the performances of the SERS chip here proposed, in terms of sensitivity, homogeneity and accuracy of the response.

4. Conclusions

An easy seed-growth approach to prepare SERS chips having high EF and very good homogeneity was here presented, based on a dense layer of silver nano-objects directly attached on a glass slide. Shape and dimensions of the nano-objects can be effectively tuned by controlling the seed-growth time, providing a high concentration of SERS hot spots on the surface. The SERS response of four kinds of chips based on different growing times were investigated, both in terms of signal enhancement and homogeneity of the response, using MMC as probe molecule. When growing time is set to 60 min, a remarkable result is obtained both in terms of EF (2×10^5) using a 532 nm laser excitation, and of good homogeneity of the SERS response with intra- and inter-maps RSD of 10% and 5%, respectively, making the SERS chips suitable for the setup of accurate analytical procedures. An analytical procedure for the detection of thiram fungicide was developed and applied to its detection on green apples peels, comparing different types of regressions for calibration. In particular, multivariate analysis based on PLS showed good repeatability and robustness (RMSECV = 0.7 ppm; RMSEP = 0.7 ppm) in the range 0–7.5 $mgkg^{-1}$, with higher accuracy for PLS (90.7%) than univariate calibration (83.4%). These results confirm that this SERS chip coupled with a PLS approach guarantees high accuracy and repeatability for thiram detection on food matrix and can be reliably used for its detection within the European law limits.

CRediT authorship contribution statement

Agnese D'Agostino: Methodology, Investigation, Data curation, Writing - original draft. **Andrea Mario Giovannozzi:** Conceptualization, Resources, Writing - review & editing, Supervision. **Luisa Mandrile:** Validation, Formal analysis, Data curation. **Alessio Sacco:** Methodology, Investigation, Data curation. **Andrea Mario Rossi:** Funding acquisition, Supervision, Writing - review & editing. **Angelo Taglietti:** Conceptualization, Writing - review & editing, Funding acquisition, Supervision.

Declaration of competing interest

The authors declare that they have no known competing financial interests or personal relationships that could have appeared to influence the work reported in this paper.

Appendix A. Supplementary data

Supplementary data to this article can be found online at https://doi.org/10.1016/j.talanta.2020.120936.

References

[1] M.F. Cardinal, E. Vander Ende, R.A. Hackler, M.O. McAnally, P.C. Stair, G.C. Schatz, R.P. Van Duyne, Expanding applications of SERS through versatile nanomaterials engineering, Chem. Soc. Rev. 46 (2017) 3886–3903, https://doi.org/10.1039/c7cs00207f.
[2] M. Kahraman, E.R. Mullen, A. Korkmaz, S. Wachsmann-Hogiu, Fundamentals and applications of SERS-based bioanalytical sensing, Nanophotonics 6 (2017) 831–852, https://doi.org/10.1515/nanoph-2016-0174.
[3] D. Cialla, A. Maerz, R. Boehme, F. Theil, K. Weber, M. Schmitt, J. Popp, Surface-enhanced Raman spectroscopy (SERS): progress and trends, Anal. Bioanal. Chem. 403 (2012) 27–54, https://doi.org/10.1007/s00216-011-5631-x.
[4] J. Chen, Y. Huang, P. Kannan, L. Zhang, Z. Lin, J. Zhang, T. Chen, L. Guo, Flexible and adhesive surface enhance Raman scattering active tape for rapid detection of pesticide residues in fruits and vegetables, Anal. Chem. 88 (2016) 2149–2155, https://doi.org/10.1021/acs.analchem.5b03735.
[5] X.-M. Lin, Y. Cui, Y.-H. Xu, B. Ren, Z.-Q. Tian, Surface-enhanced Raman spectroscopy: substrate-related issues, Anal. Bioanal. Chem. 394 (2009) 1729–1745, https://doi.org/10.1007/s00216-009-2761-5.
[6] J.-A. Huang, Y.-L. Zhang, H. Ding, H.-B. Sun, SERS-enabled lab-on-a-chip systems, Adv. Opt. Mater. 3 (2015) 618–633, https://doi.org/10.1002/adom.201400534.
[7] S.-Y. Ding, E.-M. You, Z.-Q. Tian, M. Moskovits, Electromagnetic theories of surface-enhanced Raman spectroscopy, Chem. Soc. Rev. 46 (2017) 4042–4076, https://doi.org/10.1039/c7cs00238f.
[8] A. Shiohara, Y. Wang, L.M. Liz-Marzan, Recent approaches toward creation of hot spots for SERS detection, J. Photochem. Photobiol. C 21 (2014) 2–25, https://doi.org/10.1016/j.jphotochemrev.2014.09.001.
[9] E.C. Le Ru, E. Blackie, M. Meyer, P.G. Etchegoin, Surface enhanced Raman scattering enhancement factors: a comprehensive study, J. Phys. Chem. C 111 (2007) 13794–13803, https://doi.org/10.1021/jp0687908.
[10] A.S.D.S. Indrasekara, S. Meyers, S. Shubeita, L.C. Feldman, T. Gustafsson, L. Fabris, Gold nanostar substrates for SERS-based chemical sensing in the femtomolar regime, Nanoscale 6 (2014) 8891–8899, https://doi.org/10.1039/c4nr02513j.
[11] J. Kneipp, H. Kneipp, K. Kneipp, SERS - a single-molecule and nanoscale tool for bioanalytics, Chem. Soc. Rev. 37 (2008) 1052–1060, https://doi.org/10.1039/b708459p.
[12] X.-Y. Zhang, A. Hu, T. Zhang, W. Lei, X.-J. Xue, Y. Zhou, W.W. Duley, Self-assembly of large-scale and ultrathin silver nanoplate films with tunable plasmon resonance properties, ACS Nano 5 (2011) 9082–9092, https://doi.org/10.1021/nn203336m.
[13] D. Cheng, M. He, J. Ran, G. Cai, J. Wu, X. Wang, Depositing a flexible substrate of triangular silver nanoplates onto cotton fabrics for sensitive SERS detection, Sensor. Actuator. B Chem. 270 (2018) 508–517, https://doi.org/10.1016/j.snb.2018.05.075.
[14] G. Weng, Y. Feng, J. Zhao, J. Li, J. Zhu, J. Zhao, Size dependent SERS activity of Ag triangular nanoplates on different substrates: glass vs paper, Appl. Surf. Sci. 478 (2019) 275–283, https://doi.org/10.1016/j.apsusc.2019.01.142.
[15] G. Liu, G. Duan, L. Jia, J. Wang, H. Wang, W. Cai, Y. Li, Fabrication of self-standing silver nanoplate Arrays by seed-decorated electrochemical route and their structure-induced properties, J. Nanomater. (2013), https://doi.org/10.1155/2013/365947.
[16] T. Jiang, G. Chen, X. Tian, S. Tang, J. Zhou, Y. Feng, H. Chen, Construction of long narrow gaps in Ag nanoplates, J. Am. Chem. Soc. 140 (2018) 15560–15563, https://doi.org/10.1021/jacs.8b06969.
[17] T. Jiang, X. Wang, J. Tang, S. Tang, Seed-mediated synthesis of floriated Ag nanoplates as surface enhanced Raman scattering substrate for in situ molecular detection, Mater. Res. Bull. 97 (2018) 201–206, https://doi.org/10.1016/j.materresbull.2017.08.048.
[18] C. Zhu, G. Meng, Q. Huang, Z. Huang, Vertically aligned Ag nanoplate-assembled film as a sensitive and reproducible SERS substrate for the detection of PCB-77, J. Hazard Mater. 211 (2012) 389–395, https://doi.org/10.1016/j.jhazmat.2011.07.118.
[19] T. Jiang, J. Li, L. Zhang, B. Wang, J. Zhou, Microwave assisted in situ synthesis of Ag-NaCMC films and their reproducible surface-enhanced Raman scattering signals, J. Alloys Compd. 602 (2014) 94–100, https://doi.org/10.1016/j.jallcom.2014.03.020.
[20] Y. Tian, H. Liu, Y. Chen, C. Zhou, Y. Jiang, C. Gu, T. Jiang, J. Zhou, Seedless one-spot synthesis of 3D and 2D Ag nanoflowers for multiple phase SERS-based molecule detection, Sensor. Actuator. B Chem. 301 (2019), https://doi.org/10.1016/j.snb.2019.127142.
[21] N. Abu Bakar, J.G. Shapter, M.M. Salleh, A.A. Umar, Self-assembly of high density

of triangular silver nanoplate films promoted by 3-aminopropyltrimethoxysilane, Appl. Sci. 5 (2015) 209–221, https://doi.org/10.3390/app5030209.
[22] B.N. Khlebtsov, V.A. Khanadeev, E.V. Panfilova, D.N. Bratashov, N.G. Khlebtsov, Gold nanoisland films as reproducible SERS substrates for highly sensitive detection of fungicides, ACS Appl. Mater. Interfaces 7 (2015) 6518–6529, https://doi.org/10.1021/acsami.5b01652.
[23] A. D'Agostino, A. Taglietti, P. Grisoli, G. Dacarro, L. Cucca, M. Patrini, P. Pallavicini, Seed mediated growth of silver nanoplates on glass: exploiting the bimodal antibacterial effect by near IR photo-thermal action and Ag+ release, RSC Adv. 6 (2016) 70414–70423, https://doi.org/10.1039/c6ra11608f.
[24] B. Bassi, G. Dacarro, P. Galinetto, E. Giulotto, N. Marchesi, P. Pallavicini, A. Pascale, S. Perversi, A. Taglietti, Tailored coating of gold nanostars: rational approach to prototype of theranostic device based on SERS and photothermal effects at ultralow irradiance, Nanotechnology 29 (2018), https://doi.org/10.1088/1361-6528/aab74f.
[25] A. Taglietti, Y.A.D. Fernandez, P. Galinetto, P. Grisoli, C. Milanese, P. Pallavicini, Mixing thiols on the surface of silver nanoparticles: preserving antibacterial properties while introducing SERS activity, J. Nanoparticle Res. 15 (2013), https://doi.org/10.1007/s11051-013-2047-x.
[26] B.M. Wise, N.B. Gallagher, R. Bro, J.M. Shaver, W. Windig, S.R. Koch, PLS_Toolbox, (2006) Version 4.0.
[27] E. Cara, L. Mandrile, F.F. Lupi, A.M. Giovannozzi, M. Dialameh, C. Portesi, K. Sparnacci, N. De Leo, A.M. Rossi, L. Boarino, Influence of the long-range ordering of gold-coated Si nanowires on SERS, Sci. Rep. 8 (2018), https://doi.org/10.1038/s41598-018-29641-x.
[28] W. Wei, S. Li, J.E. Millstone, M.J. Banholzer, X. Chen, X. Xu, G.C. Schatz, C.A. Mirkin, Surprisingly long-range surface-enhanced Raman scattering (SERS) on Au-Ni multisegmented nanowires, Angew. Chem. Int. Ed. 48 (2009) 4210–4212, https://doi.org/10.1002/anie.200806116.
[29] V. Peksa, P. Lebruskova, H. Sipova, J. Stepanek, J. Bok, J. Homola, M. Prochazka, Testing gold nanostructures fabricated by hole-mask colloidal lithography as potential substrates for SERS sensors: sensitivity, signal variability, and the aspect of adsorbate deposition, Phys. Chem. Chem. Phys. 18 (2016) 19613–19620, https://doi.org/10.1039/c6cp02752k.
[30] W. Wu, L. Liu, Z. Dai, J. Liu, S. Yang, L. Zhou, X. Xiao, C. Jiang, V.A.L. Roy, Low-cost, disposable, flexible and highly reproducible screen printed SERS substrates for the detection of various chemicals, Sci. Rep. 5 (2015), https://doi.org/10.1038/srep10208.
[31] A. Sacco, S. Mangino, C. Portesi, E. Vittone, A.M. Rossi, Novel approaches in tip-enhanced Raman spectroscopy: accurate measurement of enhancement factors and pesticide detection in tip dimer configuration, J. Phys. Chem. C 123 (40) (2019) 24723–24730, https://doi.org/10.1021/acs.jpcc.9b07016 0 (n.d.) null.
[32] X. Lu, Y. Huang, B. Liu, L. Zhang, L. Song, J. Zhang, A. Zhang, T. Chen, Light-controlled shrinkage of large-area gold nanoparticle monolayer film for tunable SERS activity, Chem. Mater. 30 (2018) 1989–1997, https://doi.org/10.1021/acs.chemmater.7b05176.
[33] Y. Huang, A. Dandapat, D.-H. Kim, Covalently capped seed-mediated growth: a unique approach toward hierarchical growth of gold nanocrystals, Nanoscale 6 (2014) 6478–6481, https://doi.org/10.1039/c4nr00587b.
[34] Y. Huang, L. Dai, L. Song, L. Zhang, Y. Rong, J. Zhang, Z. Nie, T. Chen, Engineering gold nanoparticles in compass shape with broadly tunable plasmon resonances and high-performance SERS, ACS Appl. Mater. Interfaces 8 (2016) 27949–27955, https://doi.org/10.1021/acsami.6b05258.
[35] T. Cajka, K. Riddellova, P. Zomer, H. Mol, J. Hajslova, Direct analysis of dithiocarbamate fungicides in fruit by ambient mass spectrometry, Food Addit. Contam. A 28 (2011) 1372–1382, https://doi.org/10.1080/19440049.2011.590456.
[36] L. Zhang, B. Wang, G. Zhu, X. Zhou, Synthesis of silver nanowires as a SERS substrate for the detection of pesticide thiram, Spectrochim. Acta A 133 (2014) 411–416, https://doi.org/10.1016/j.saa.2014.06.054.
[37] S. Sanchez-Cortes, C. Domingo, J.V. Garcia-Ramos, J.A. Aznarez, Surface-enhanced vibrational study (SEIR and SERS) of dithiocarbamate pesticides on gold films, Langmuir 17 (2001) 1157–1162, https://doi.org/10.1021/la001269z.
[38] J. Zhu, Q. Chen, F.Y.H. Kutsanedzie, M. Yang, Q. Ouyang, H. Jiang, Highly sensitive and label-free determination of thiram residue using surface-enhanced Raman spectroscopy (SERS) coupled with paper-based microfluidics, Anal. Methods. 9 (2017) 6186–6193, https://doi.org/10.1039/c7ay01637a.
[39] L. Mandrile, A.M. Giovannozzi, F. Durbiano, G. Martra, A.M. Rossi, Rapid and sensitive detection of pyrimethanil residues on pome fruits by Surface Enhanced Raman Scattering, Food Chem. 244 (2018) 16–24, https://doi.org/10.1016/j.foodchem.2017.10.003.